0026-895X/11/7906-953–963$25.00
MOLECULAR PHARMACOLOGY
Vol. 79, No. 6
70409/3692038
*Mol Pharmacol* 79:953–963, 2011
*Printed in U.S.A.*




# RNA-Induced Silencing Complex-Bound Small Interfering RNA Is a Determinant of RNA Interference-Mediated Gene Silencing in Mice[S]

Jie Wei, Jeffrey Jones, Jing Kang, Ananda Card, Michael Krimm, Paula Hancock,Yi Pei, Brandon Ason, Elmer Payson, Natalya Dubinina, Mark Cancilla, Mark Stroh, Julja Burchard, Alan B. Sachs, Jerome H. Hochman, W. Michael Flanagan, and Nelly A. Kuklin

*Sirna Therapeutics, a wholly owned subsidiary of Merck & Co, Inc., San Francisco, California (J.W., J.J., J.K., A.C., M.K., B.A., E.P., N.D., M.C., J.B., A.B.S., W.M.F., N.A.K.); and RNA Delivery (P.H., Y.P.) and Clinical PK/PD, Merck Research Laboratories, West Point, Pennsylvania (M.S., J.H.H.)*

Received December 7, 2010; accepted March 21, 2011

## ABSTRACT

Deeper knowledge of pharmacokinetic and pharmacodynamic (PK/PD) concepts for RNA therapeutics is important to streamline the drug development process and for rigorous selection of best performing drug candidates. Here we characterized the PK/PD relationship for small interfering RNAs (siRNAs) targeting luciferase by examining siRNA concentration in plasma and liver, the temporal RNA-induced silencing complex binding profiles, mRNA reduction, and protein inhibition measured by noninvasive bioluminescent imaging. A dose-dependent and time-related decrease in bioluminescence was detected over 25 days after a single treatment of a lipid nanoparticle-formulated siRNA targeting luciferase messenger RNA. A direct relationship was observed between the degree of in vivo mRNA and protein reduction and the Argonaute2 (Ago2)-bound siRNA fraction but not with the total amount of siRNA found in the liver, suggesting that the Ago2-siRNA complex is the key determinant of target inhibition. These observations were confirmed for an additional siRNA that targets endogenously expressed Sjögren syndrome antigen B (Ssb) mRNA, indicating that our observations are not limited to a transgenic mouse system. Our data provide detailed information of the temporal regulation of siRNA liver delivery, Ago2 loading, mRNA reduction, and protein inhibition that are essential for the rapid and cost-effective clinical development of siRNAs therapeutics.

## Introduction

RNA interference (RNAi) is an evolutionarily conserved mechanism involved in regulation of gene expression (Tuschl, 2001; Scherr and Eder, 2007). RNAi uses small double-stranded RNAs known as small interfering RNAs (siRNAs) to induce site-specific cleavage of an mRNA transcript, leading to its subsequent degradation. Synthetic siRNAs hold tremendous therapeutic potential because of their ability to induce potent, persistent, and specific suppression of disease-causing genes. As evidence for this, it is noteworthy that the first clinical trial of an RNAi-based drug started only 3 years after the initial discovery of RNAi in mammalian cells (Elbashir et al., 2001). Several RNAi-based drugs are currently under clinical evaluation (Watts et al., 2008). As this area matures, so will the processes by which siRNA clinical candidates are chosen. In particular, a detailed understanding of the pharmacokinetic (PK) fate and pharmacodynamic (PD) effect of siRNAs in vivo will provide a rigorous basis for candidate selection and therefore improve the performance of the candidate in clinical studies. (Meibohm and Derendorf, 2002; Bartlett and Davis, 2006; Gabrielsson et al., 2009).

Effective delivery remains a major technical challenge associated with siRNA therapeutics (Sepp-Lorenzino and Ruddy, 2008). Systemic delivery of siRNAs involves multiple steps, including siRNA biodistribution, cellular interaction

This work was supported by Merck and Co., Inc.
Article, publication date, and citation information can be found at http://molpharm.aspetjournals.org.
doi:10.1124/mol.110.070409.
[S] The online version of this article (available at http://molpharm.aspetjournals.org) contains supplemental material.

**ABBREVIATIONS:** RNAi, RNA interference; siRNA, small interfering RNA; PK, pharmacokinetic; PD, pharmacodynamic; RISC, RNA-induced silencing complex; RSV, respiratory syncytial virus; LNP, lipid nanoparticle; CMV, cytomegalovirus; AUC, area under the curve; RT-PCR, reverse transcription-polymerase chain reaction; qPCR, quantitative PCR; *GAPDH*, glyceraldehyde 3-phosphate dehydrogenase; UC3, scrambled universal control; PBS, phosphate-buffered saline; Ago2, Argonaute2; Luc, Luciferase; Ssb, Sjögren syndrome antigen B; MGBNFQ, minor groove binder nonfluorescent quencher.

with the delivery vehicle, intracellular uptake, endosomal release, Clp-1 phosphorylation, and binding of siRNAs to RNA-induced silencing complex (RISC) (Gilmore et al., 2006; Parker et al., 2006; Vaishnaw et al., 2010). RISC is a complex of multiple proteins including Argonaute 2 (Ago2), Dicer, and transactivating response RNA-binding protein. Ago2 is the "slicer" responsible for cleaving the mRNA transcript. During siRNA-RISC assembly, the siRNA duplex is unwound, and one strand (i.e., the passenger strand) is degraded, whereas the other strand (i.e., the guide strand) facilitates target mRNA degradation (Matranga et al., 2005; Lima et al., 2009). Inefficiencies in any of these steps could hypothetically mitigate the PD effect of an siRNA therapy.

Few clinical PK/PD studies using siRNAs have been reported. Davis et al. (2010) reported PD results from the first phase I trial of a siRNA systemically delivered to cancer patients using a targeted nanoparticle. Tumor biopsies were analyzed from three different patients. All biopsies after siRNA treatment showed reduced mRNA expression for the target ribonucleotide reductase M2. Tumor biopsies from one patient who received the highest dose of nanoparticle-formulated siRNA showed an mRNA fragment consistent with the siRNA-directed site-specific Ago2 cleavage of ribonucleotide reductase M2 transcript. This report provided the first evidence for the RNAi mechanism of action in humans. Unfortunately, the concentration of the siRNA delivered to the tumor was not quantified, and no PK and PD relationship could be established. Reports from two phase I studies evaluated the pharmacokinetics of ALN-RSV01, a siRNA against respiratory syncytial virus (RSV) (DeVincenzo et al., 2008). However, because ALN-RSV01 was administered intranasally to patients, systemic exposure to the siRNA was minimal. Furthermore, no siRNA-mediated inhibition of the RSV target was evaluated.

Although it is understandable that patient-based siRNA PK and PD relationships are incomplete, it is surprising that there is a lack of siRNA-focused preclinical PK and PD reports, especially with the advent of small-animal molecular imaging as a means for evaluating PD (Willmann et al., 2008). Bioluminescent images captured over time can replace the need to perform invasive techniques on laboratory animals (Safran et al., 2003; Bartlett and Davis, 2007; John et al., 2007). Bartlett and Davis (2007) investigated the impact of tumor-specific targeting and dose schedule on tumor growth. They found that dose, dose frequency, and total amount of siRNA in the tissue had no direct effect on tumor growth inhibition; however, it is unclear from these experiments whether siRNA dose and frequency resulted in increased siRNA delivery to the tumor and enhanced target inhibition. Clearly, a comprehensive understanding of the PK and PD of the siRNA could help explain the lack of a dose response in that preclinical in vivo model.

Here, we report the results of a quantitative PK and PD analysis using lipid nanoparticle (LNP)-formulated siRNA from 5 min to 25 days after intravenous administration. This study evaluated the plasma and tissue concentrations as well as the intensity and duration of the pharmacologic effects of an siRNA-targeting luciferase in a transgenic mouse model designed to constitutively express luciferase in the liver. The results of this study provide a detailed time course of siRNA plasma and liver concentrations, RISC loading, silencing of the target mRNA transcript, and protein inhibition. The PK/PD relationship of siRNAs reported here will enable more informed decisions in selecting the optimal siRNA chemistry, delivery vehicle, dose, and schedule for the evaluation of siRNA molecules destined for the clinic.

## Materials and Methods

**siRNA Design, Synthesis, and Sequence.** Chemically modified siRNAs contained either ribo (r), deoxy (d), fluoro (flu), or O-methyl (ome) 2′ modifications as described previously (Zou et al., 2008). The passenger strand contains an inverted abasic cap (iB) where indicated. siRNAs were synthesized as described previously (Wincott, 2001). The siRNA sequences and modification are as follows.

The Luc(80) siRNA consisted of the following passenger strand: 5′-iB;dA;fluU;dA;dA;dG;dG;fluC;fluU;dA;fluU;dG;dA;dA;dG;dA;dG;dA;fluU;dA;dT;dTiB-3′ and guide strand: 5′-rU;rA;rU;fluC;fluU;fluC;fluU;fluU;fluC;omeA;fluU;omeA;omeG;fluC;fluC;fluU;fluU;omeA;fluU;omeU;omeU-3′.

The Ssb(291) siRNA consisted of the following passenger strand: 5′-iB;dA;fluC;dA;dA;fluC;dA;dG;dA;fluC;fluU;fluU;fluU;dA;dA;fluU;dG;fluU;dA;dA;dT;dT;iB-3′ and guide strand: 5′-rU;rU;rA;fluC;omeA;fluU;fluU;omeA;omeA;omeA;omeG;fluU;fluC;fluU;omeG;fluU;fluU;omeG;fluU;omeU;omeU-3′.

UC3 was a scrambled version of a published luciferase siRNA, screened for matches to known genes. Passenger strand: 5′-iB;dG;fluU;dA;fluU;dG;dA;fluC;fluC;dG;dA;fluC;fluU;dA;fluC;dG;fluC;dG;fluU;dA;dT;dT;iB-3′. Guide strand: 5′-rU;rA;rC;omeG;fluC;omeG;fluU;omeA;omeG;fluU;fluC;omeG;omeG;fluU;fluC;omeA;fluU;omeA;fluC;omeU;omeU-3′

**siRNA Delivery and Formulation.** Lipid nanoparticles were made using the cationic lipid 2-{4-[(3b)-cholest-5-en-3-yloxy]-octyl}-*N*,*N*-dimethyl-3-[(9*Z*,12*Z*)-octadeca-9,12-dien-1-yloxy]propan-1-amine (Merck and Co., Inc., Whitehouse Station, NJ), cholesterol (Northern Lipids, Burnaby, BC, Canada), and monomethoxypolyethyleneglycol-1,2-dimyristoylglycerol (NOF Corporation, Tokyo, Japan) at a 60:38:2 M ratio, respectively.

**In Vivo Studies.** All experimental animal procedures adhered to a protocol approved by the Institutional Animal Care and Use Committee and were consistent with local, state, and federal regulations and the journal requirements. Studies were performed in homozygous Rosa26-LSL-luciferase transgenic mice as described previously (Tao et al., 2010). The mice were licensed from the Dana-Farber Cancer Institute and bred at Taconic Farms (Hudson, NY). Rosa26 mice consist of a FVB.129S6 (B6) genetic background containing a luciferase (Luc) cDNA preceded by a loxp-stop-loxp (L-S-L) in the *Rosa26* locus (Safran et al., 2003). Liver-specific expression of luciferase was induced by intravenous injection of replication-deficient recombinant *Cre* adenovirus, Ad-CMV-*Cre* (Vector Biolabs, Philadelphia, PA) that excised the stop sequence, thereby placing the luciferase gene under control of the *Rosa26* locus (Safran et al., 2003). The optimal dose of recombinant *Cre* adenovirus capable of inducing maximum luciferase expression was determined to be 2 to 3 $\times$ $10^9$ plaque-forming units. Steady-state luciferase expression was reached ~2 weeks after injection of the virus. The bioluminescence emanating from the livers of Ad-CMV-*Cre*–induced Rosa26-LSL-Luc mice persisted for at least 2 months without perceptible decrease in bioluminescence. For RNA analysis, animals were euthanized, and both plasma samples and a section of the right medial lobe of the liver were collected from each animal. Plasma samples were stored at −80°C before use. The excised liver sections were placed in RNALater at 4°C for mRNA quantification and stored at −80°C or flash-frozen for siRNA quantification and stored at −80°C before use.

**Bioluminescence Measurement and Analysis.** Bioluminescence was measured using a Xenogen IVIS (Alameda, CA) imaging system as described previously (Tao et al., 2010). In brief, mice were injected intraperitoneally with 0.2 ml of luciferase substrate D-luciferin (Caliper Life Sciences, Hopkinton, MA) solution (20 mg/ml in PBS) 10 min before imaging. Mice were anesthetized using 3% iso-

flurane with the oxygen flow at 1 l/min for 3.5 min. Images were taken using a 20-cm field of view and an exposure time of 1 s. Bioluminescent images were displayed by overlaying a bioluminescence intensity representative pseudocolor image (blue representing the lowest intensity and red representing the highest intensity) on a gray-scale mouse image to generate a two-dimensional picture of the distribution of bioluminescence in the mouse liver. Bioluminescence values were calculated by measuring the photon flux (photons per second) in the region of interest surrounding the bioluminescence signal emanating from the mice with the Living Image software (Xenogen Corp, Alameda, CA). Bioluminescence reduction after luciferase siRNA treatment was evaluated by calculating the luminescence intensity values (photons per second per centimeter squared per steradian) at the time of measurement relative to values of pretreatment (day 0), and presented as relative bioluminescence ($-\log_2$-fold change or percentage reduction).

**Pharmacodynamic Half-Life Calculation.** Time dependence of $\log_2$-fold changes in luciferase bioluminescence as a result of siRNA silencing and its subsequent decay were fitted with the following equation: $\log_2(\text{bioluminescence}) = k_1 \cdot e^{-k2t} + k3 \cdot e^{-k4t}$. In this sum of exponentials, the second term represents the decay of the preformed pool of luciferase protein, whereas the first term represents the decay of maximum silencing of luciferase transcript. For simplicity, both protein expression and silencing are assumed to be maximal before the first measurement at day 1. Half-life ($t_{1/2}$ or recovery time) is calculated from the silencing decay term: $t_{1/2} = \ln(2)/k_2$.

**Pharmacodynamic Durability.** Area under the curve (AUC) was calculated via the trapezoid method using Prism (GraphPad Software, La Jolla, CA). In brief, vertical lines are dropped from each point to the baseline, and diagonals are drawn between each pair of points to form trapezoids. The areas of the trapezoids are calculated as $(X2 - X1) \times (Y2 + Y1)/2$ and then the areas of all trapezoids are summed, resulting in the AUC.

**Quantification of mRNA Reduction.** Total RNA was isolated from liver samples using RNeasy96 Universal Tissue Kit (QIAGEN, Valencia, CA) following the product protocol. Approximately 30 mg of liver was homogenized using a TissueLyser Beadmill (QIAGEN) for 20 min at 25 Hz in 750 $\mu$l of Qiazol lysis reagent (QIAGEN). An on-column DNase I treatment was performed before RNA elution. Reverse transcription polymerase chain reaction (RT-PCR) was performed using 350 ng of RNA and the TaqMan Gene Expression and Cells-to-CT Kit (Applied Biosystems, Foster City, CA) according to the product protocol. Real-time qPCR was performed in a 10-$\mu$l reaction volume using the 7900 HT Fast Real-Time PCR System (Applied Biosystems). All reactions were conducted in duplicate. *GAPDH* (glyceraldehyde 3-phosphate dehydrogenase) was used as an endogenous control gene.

Relative quantification of mRNA was performed using the comparative Ct ($2^{-\Delta\Delta Ct}$) method (Livak and Schmittgen, 2001). In brief, the endogenous gene *Gapdh* was used as an internal control gene to normalize each PCR for the amount of RNA added in the reverse transcription reactions and presented as $\Delta Ct$ ($Ct_{target} - Ct_{Gapdh}$); therefore, the Ct value of target gene was normalized to the Ct value of *Gapdh* for each sample. The relative expression level of target gene of interest after siRNA treatment was evaluated by normalizing the mean $\Delta Ct$ ($Ct_{target} - Ct_{Gapdh}$) value of siRNA treated group to the mean $\Delta Ct$ ($Ct_{target} - Ct_{Gapdh}$) value of PBS treated negative control group, presented as $\Delta\Delta Ct$ ($\Delta Ct_{siRNA\text{-}treated} - \Delta Ct_{PBS\text{-}treated}$), representing $-\log_2$-fold change, or as $100 \times (1–2^{-\Delta\Delta Ct})$, representing percentage of mRNA reduction.

**In Vivo siRNA Quantification.** The siRNA concentration of the plasma and liver samples was determined using the following sample preparation and stem-loop RT-PCR and real-time qPCR methods, modified from a method described previously (Chen et al., 2005). Liver samples were homogenized using 500 $\mu$l of Qiazol lysis reagent per 50 mg of tissue and a Genogrinder 2000 (Spex Certiprep Inc., Metuchen, NJ) with a 5/32-in stainless steel bead at 1300 strokes/min for 5 min. Samples were subsequently incubated at 37°C for 30 min. Plates were spun briefly, and the homogenate was diluted 1:1000 in Tris-EDTA buffer. The concentration of siRNA was determined using an eight-point standard curve generated by spiking a 0.1% dilution of treatment-naive mouse liver homogenate or plasma with a 10-fold serial dilution of naked siRNA starting at 100 ng/ml.

The RT primer sequence of the luciferase siRNA was 5′-GTCGTATCCAGTGCAGGGTCCGAGGTAGGCTACAGGCACGCACTGGATACGACAAATAAG-3′. The annealing step was performed in a 16-$\mu$l reaction containing 25 nM stem-loop RT primer and 10 $\mu$l of diluted homogenate. The reaction was incubated at 95°C for 5 min, 80°C for 2 min, 70°C for 2 min, 60°C for 2 min, and 45°C for 2 min with a 4°C hold. RT-PCR was performed using the TaqMan MicroRNA Reverse Transcription Kit (Applied Biosystems) per the product protocol but using only 0.5 $\mu$l per reaction of MultiScribe RT enzyme.

Real-time qPCR was performed in a 20-$\mu$l reaction volume using a 7500 Fast Real-Time PCR System (Applied Biosystems). All reactions were run in triplicate. The forward primer sequence was 5′-CGCGCGTATCTCTTCATAGC-3′. The reverse primer sequence was 5′-AGTGCAGGGTCCGAG-3′. The probe sequence was 5′-6FAM-CACGCACTGGATAC-MGBNFQ-3′.

The same procedures were applied for Ssb siRNA quantification. The RT primer sequence for Ssb siRNA was 5′- GTCGTATCCAGTGCAGGGTCCGAGGTATTCGCACTGGATACGACAAACAACAGA-3′. The forward primer for Ssb siRNA was 5′-CGCGCGTTACATTAAAGTC-3′. The reverse primer for Ssb siRNA is 5′-AGTGCAGGGTCCGAG-3′. The probe sequence for Ssb siRNA is 5′-6FAM-TCGCACTGGATACGACAAACAACA-MGBNFQ-3′. All primers were obtained from Integrated DNA Technologies (Coralville, IA), and probes were obtained from Applied Biosystems. siRNA concentrations were calculated according to the detected linear regression between Ct value and log siRNA concentration from standards.

**Mouse Ago2 Immunoprecipitation Assay.** The Ago2 immunoprecipitation assay was performed as described previously (Chen et al., 2005; Pei and Tuschl, 2006). In brief, frozen liver samples (~100 mg) were homogenized using pellet pestle with 0.6 ml of 0.5% Triton X-100 lysis buffer on ice. The Ago2 pull-down from the liver lysate was performed by immunoprecipitation with anti-mouse Ago2 antibody (Wako Laboratory Chemicals, Richmond, VA) and Dynabeads protein G (Invitrogen, Carlsbad, CA). The IgG pull-down for nonspecific siRNA binding evaluation was performed with normal mouse IgG (Santa Cruz Biotechnology, Santa Cruz, CA). The amounts of guide strand siRNA and miR16 that coimmunoprecipitated with Ago2 were quantified by stem-loop RT-PCR as described above. To determine the concentrations of miR16 bound to Ago2, eight 5-fold serial dilutions of synthetic RNA oligonucleotides representing miRNAs, including miR16 in mirVana miRNA reference panel V9.1 (Applied Biosystems/Ambion, Austin, TX) starting at 0.2 fmol/$\mu$l, were spiked into the same Cell-to-Ct lysis and stop buffer (Applied Biosystems) used in the final elution step of the Ago2 immunoprecipitation assay. Calculating the linear regression between Ct value and log siRNA concentration from siRNA standards enabled the determination of the concentration of siRNA and miR16 in each sample. To account for immunoprecipitation efficiency, the amount of siRNA associated to Ago2 was normalized to endogenous miR16 associated to Ago2 because miR16 is tightly associated with RISC (Tang et al., 2008) and indiscriminately incorporated into Ago1 through Ago4 (Meister et al., 2004). The data are presented as the copy number ratio of siRNA guide strand to miR16.

**Immune Blot Analysis.** Whole-cell liver lysates were normalized for total protein concentration and separated by gel electrophoresis. Protein was blotted onto polyvinylidene fluoride membranes, blocked with 1% casein, and probed with a monoclonal antibody to Ago2 (Cell Signaling Technology, Danvers, MA) and a polyclonal antibody to $\alpha$-tubulin (Cell Signaling Technology) primary antibodies. Primary antibodies were detected with horseradish peroxidase-conjugated secondary antibody (Cell Signaling Technology) and visualized by enhanced chemiluminescence.

## Results

**A Noninvasive In Vivo Model for Monitoring siRNA Pharmacodynamics in Real Time.** As previously reported, mice containing a luciferase gene preceded by a *loxp*-stop-*loxp* in the *Rosa26* locus were used to investigate whether bioluminescence can serve as a noninvasive model for monitoring RNAi in vivo (Tao et al., 2010). Rosa26-LSL-Luciferase mice were injected intravenously with *Cre* recombinase expressing adenovirus to induce the luciferase expression in liver and subsequently used for the evaluation of siRNA-mediated in vivo gene silencing (Fig. 1A). Mice were dosed with luciferase siRNA, and the duration of gene silencing was monitored by noninvasive bioluminescence system (Fig. 1B). siRNA-mediated inhibition of in vivo bioluminescence and decreased mRNA levels were correlated, indicating that bioluminescence can serve as a noninvasive model for monitoring mRNA knockdown (Fig. 1C; $R^2 = 0.80$, $P < 0.0001$, $n = 100$).

We confirmed the work of Tao et al. (2010) for the utility of the model by showing a linear correlation between bioluminescence and luciferase mRNA using four different time points and five different concentrations of luciferase siRNA. In addition, we evaluated the effect of 2 irrelevant siRNAs [a scrambled universal control (UC3) siRNA and the Ssb siRNA] on in vivo luminescence (Supplemental Figs. 1 and 2). Our results demonstrate that both the raw luminescence data (Supplemental Fig. 1, A and B) and luminescence data normalized to the pretreatment value per mouse (Supplemental Fig. 1C) for Ssb-, UC3-, and PBS-treated groups are not significantly different from each other at the $p < 0.01$ using Kruskal-Wallis test (nonparametric ANOVA). These data demonstrate lack of a nonspecific effect of irrelevant

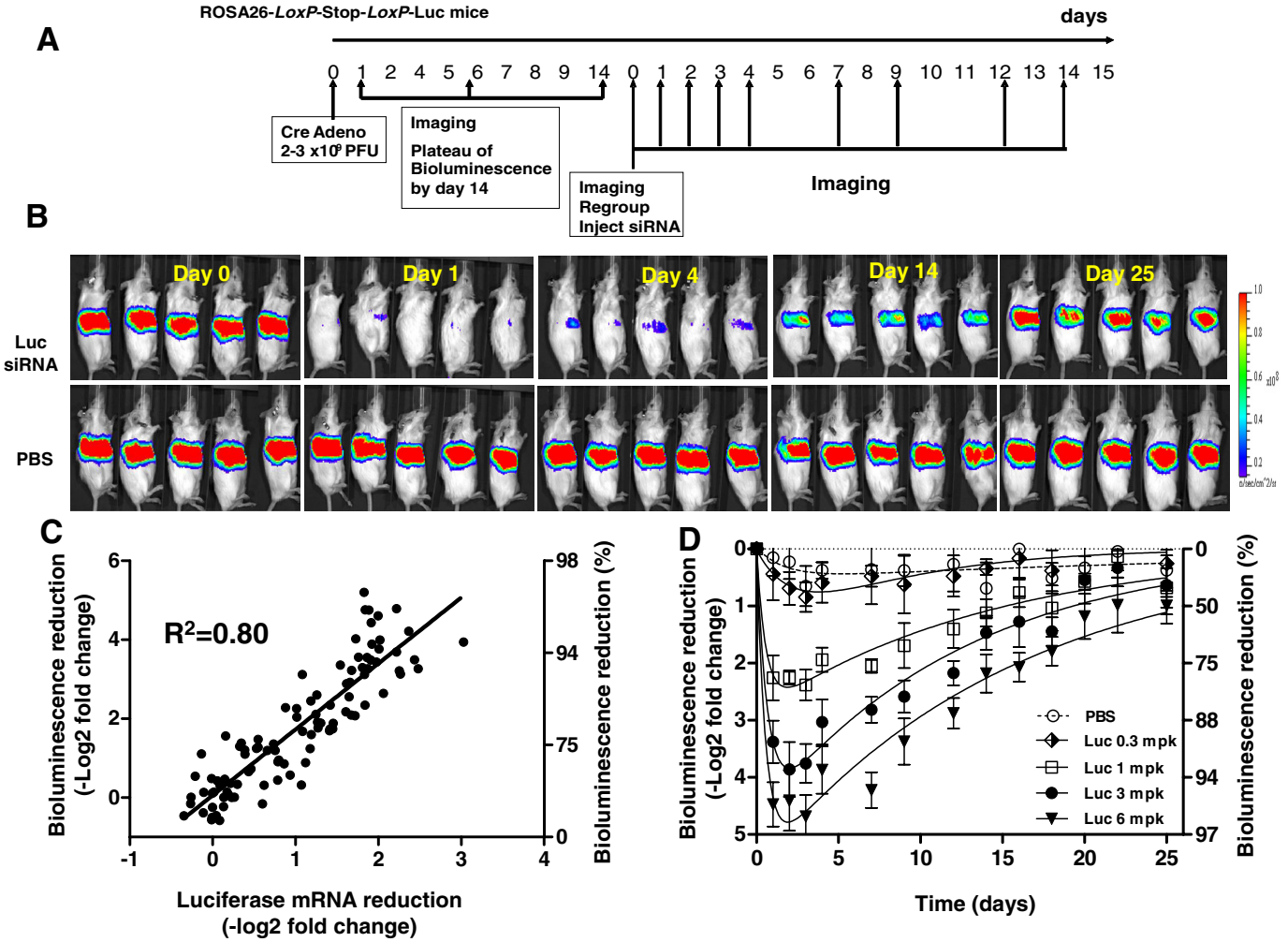


**Fig. 1.** In vivo siRNA-mediated gene silencing was monitored by noninvasive bioluminescence imaging. A, experimental design schematic. Liver-specific luciferase expression was induced in Rosa26-*loxp*-stop-*loxp*-Luc mice by the injection of Ad-CMV-Cre. Two weeks after luciferase induction, all mice were imaged and randomized based on their bioluminescence. Mice were intravenously injected with 0.3, 1, 3, or 6 mg/kg LNP-formulated siRNA targeting luciferase mRNA. Bioluminescence was measured on days 0 (pretreatment) and 1 to 4 (post-treatment), and observed twice a week to day 25. B, visual representation of bioluminescence imaging of mice after administration of luciferase siRNA at 3 mg/kg. Images were taken at day 0 (pretreatment) and days 1, 4, 14, and 25 (post-treatment) and displayed by overlaying the bioluminescence values representative pseudocolor image (blue representing the lowest intensity and red representing the highest intensity, $0.16 \times 10^8$-$1.0 \times 10^8$ p/sec/cm$^2$/sr), on the grayscale mouse image. C, Correlation between bioluminescence ($-\log_2$-fold change or percentage reduction) and luciferase mRNA inhibition ($-\log_2$-fold change). Coefficient of determination ($R^2$) equals 0.80. Each data point represents one mouse ($n = 100$). D, Dose-dependent luciferase siRNA-mediated reduction in bioluminescence ($-\log_2$-fold change or percentage reduction) was monitored over 25 days. Mice were intravenously injected with 0.3, 1, 3, or 6 mg/kg lipid nanoparticle (LNP)-formulated siRNA-targeting luciferase mRNA. Each data point represents the mean ± S.D. based on five mice per group. The solid lines represent double exponential fit of the $-\log_2$-fold change of luminescence to day 0.

siRNA on bioluminescence. For subsequent analysis, we used PBS as our negative control.

After we confirmed the utility of the model, we next investigated the pharmacological effect of varying the luciferase siRNA dose. Maximum inhibition of bioluminescence was seen by day 3 for all siRNA doses. Bioluminescence recovery to the initial predose steady-state levels was dose-dependent and, for 3 and 6 mg/kg doses, occurred after 25 days (Fig. 1D). The pharmacologic effect was directly correlated with the dose of siRNA administered. The PD half-life of the chemically modified siRNA was determined by calculating the rate of bioluminescence recovery. Except for the 0.3 mg/kg dose, which showed minimal biological activity, the siRNA PD half-life for all other doses was similar (overlapping 95% confidence intervals), indicating that the loss of biological siRNA-mediated activity was dose-independent (Table 1). For the 3 mg/kg dose, the average $t_{1/2}$ was outside of the confidence interval of the 6 mg/kg dose. However, the confidence intervals for 3 and 6 mg/kg doses overlap. An extra sum-of-squares F-test analyses rejected the 3 mg/kg dose as being different from the other groups at the $p > 0.01$ significance level (Table 1).

Because clinical dose schedules are dependent on the duration of action of the therapeutic administered, we examined luciferase siRNA duration of action. The siRNA-mediated duration of action was measured by the AUC that combines both maximum target inhibition and the PD half-life of the siRNA. Luciferase siRNA-dependent duration of action was determined by measuring bioluminescence over the course of the experiment (25 days). As shown in Table 1, the duration of the PD effect increased with increasing siRNA concentrations. Because the PD half-life of the chemically modified luciferase siRNA was similar for all doses, the siRNA biological durability, in this case, was driven by maximum target inhibition. Different siRNAs targeting the same mRNA as well as different chemical modification patterns applied to siRNAs will influence maximum silencing, the PD half-life of the siRNA, and, thus, siRNA durability.

**Gene Silencing Correlates with the Amount of siRNA Bound to Ago2.** To further understand the relationship between siRNA dose and target silencing, we examined the level of bioluminescence, the amount of siRNA present in the liver, and the amount of siRNA bound to Ago2 at various time points. Mice were imaged at baseline (predose) and subsequently sacrificed at different days after the injection of increasing doses of the luciferase-targeting siRNA (Fig. 2). Dose-dependent responses were observed for all measurements, luciferase-protein silencing approaching a plateau near the 6 mg/kg dose (Fig. 2, A–C). Compared with day 1, substantially lower levels of siRNA were detected in the liver at day 3, with a further decrease seen by day 7 (Fig. 2A). The liver siRNA concentrations were below the threshold of detection for the two lower dose groups at day 14 and for all dose groups at day 25. Despite the rapid decline in the total amount of siRNA found in the liver, the fraction of siRNA bound to Ago2 seemed more persistent, with small, but detectable levels seen out to day 25 (Fig. 2B). The siRNA amount detected from nonspecific mouse IgG pull-down assay control was marginal compared with siRNA from Ago2 pull-down assay (data not shown). The percentage of siRNA bound to Ago2 increased with time compared with total siRNA in liver. At days 1 and 3, the amount of siRNA bound to Ago2 was approximately 15 and 50%, respectively, of the total siRNA in liver. After day 7, more than 90% of the total siRNA was bound to Ago2 (Fig. 2, A and B), suggesting that RISC-bound siRNA persists long after nonproductive liver-associated siRNAs are eliminated and accounts for the observed target silencing at day 14 and 25 (Fig. 2C). These data suggest that Ago2 binding and possibly the subcellular compartments in which the siRNA-Ago2 complexes are located protect the siRNA from intracellular nucleases, resulting in increased siRNA stability and prolonged siRNA-mediated silencing. This conclusion is reflected in the strong relationship ($R^2 = 0.87$, $n = 125$) between luciferase protein inhibition as measured by bioluminescence and the fraction of siRNA bound to Ago2 over time (Fig. 2D). In contrast, a weaker correlation between luciferase protein inhibition and total siRNA in the liver was observed ($R^2 = 0.59$, $n = 105$) (Fig. 2E).

To evaluate whether the above observations are widely applicable, a similar experiment employing an siRNA that targets Ssb [Ssb(291)] was performed in C56BL/6 mice. Again, the total amount of siRNA found in the liver decreased at a faster rate relative to the Ago2-bound siRNA fraction (Fig. 3, A and B). Maximum Ssb knockdown was observed at 3 mg/kg and persisted through day 7 (Fig. 2C). A robust correlation ($R^2 = 0.91$, $n = 90$) across all time points and doses was seen only for mRNA silencing and the fraction bound by Ago2 (Fig. 3D). In contrast, weaker correlation between total Ssb siRNA in liver and mRNA silencing was observed during the time course of the experiment ($R^2 = 0.23$, $n = 80$) (Fig. 3E).

For both Ssb and luciferase siRNA at doses 1 to 6 mg/kg, the concentration of Ago2-bound siRNAs increased with an escalating dose of siRNA (Figs. 2B and 3B), even beyond doses that achieved substantial mRNA knockdown (Figs. 2C and 3C). Tukey nonparametric pair-wise post-test analysis demonstrated that luciferase siRNA Ago2 binding at 3 mg/kg is significantly different from Ago2 binding at 6 or 9 mg/kg at 1, 3, and 7 days after delivery ($p < 0.05$) (Fig. 2B). Silencing

TABLE 1
Duration of pharmacodynamic effect measured as decrease of bioluminescence over time
AUC and $t_{1/2}$ were calculated over 25 days. Bioluminescence $-\log_2$-fold change represents bioluminescence reduction at day 3. An extra sum-of-squares F-test was performed. Bioluminescence was measured at day 3.

| Dose of siRNA | Bioluminescence Change | PD Effect $t_{1/2}$ | Duration of the PD Effect AUC |
|---|---|---|---|
| | *$-log_2$-fold (%)* | *days (95% CI)* | *relative bioluminescence × days* |
| 0.3 mg/kg | 0.8 (43) | 5.3 (2.7, 208) | 9.1 |
| 1 mg/kg | 2.4 (81) | 10.0 (8.6,12.0) | 32.1 |
| 3 mg/kg | 3.8 (93)* | 8.6 (7.6, 9.9) | 47.3 |
| 6 mg/kg | 4.7 (96) | 10.7 (9.6,12.1) | 66.0 |

AUC = area under the curve; CI = confidence interval; PD = pharmacodynamic; $t_{1/2}$ = half-life
* F-test rejects 3 mg/kg being different from the others within the same experiment at the $P > 0.01$ significance level.

of luciferase protein, however, is not significantly different at these doses on these days (Fig. 2C).

Likewise, Ssb siRNA Ago2 binding at 3 mg/kg is significantly different from Ago2 binding at 6 or 9 mg/kg at 1 and 3 days after delivery ($p < 0.05$) (Fig. 3B). In contrast, silencing Ssb mRNA is not significantly different at these doses on these days (Fig. 3C). We note that SSB is ubiquitously expressed and that there might be some dynamic range compression in measurement of SSB mRNA reduction. We did not observe a significant difference between Ago2 binding for the same doses at day 7.

The statistical analysis suggests that bioluminescence or mRNA knockdown between the 3, 6, and 9 mg/kg dose groups were reaching a plateau. There was, however, a statistically significant difference for the amount of siRNA bound by Ago2 for these dose groups. Based on a range of siRNA doses, time-course studies, and quantitation of both Ssb and luciferase siRNAs bound to Ago2, we estimated that 280 to 1260 siRNA guide strands per hepatocyte resulted in 50% target inhibition of Ssb and luciferase, respectively (Supplemental Table 1).

The Ago2 binding for the 6 and 9 mg/kg dose groups was not statistically significantly different for both luciferase and Ssb siRNA. We are unable to raise the dose 2-fold (from 6 to 12 mg/kg) because a dose ≥12 mg/kg induces in vivo toxicity.

To ensure that the differences in Ago2 binding among the various siRNA doses were dependent on dose and not technical artifacts of the miR16 normalization or Ago2 immunoprecipitation, the amount of miR16 bound to Ago2 and the efficiency of Ago2 immunoprecipitation was examined. Analysis of miR16 bound to Ago2 showed no change over the range of luciferase or Ssb siRNA doses (Supplemental Fig. 3). Likewise, the efficiency

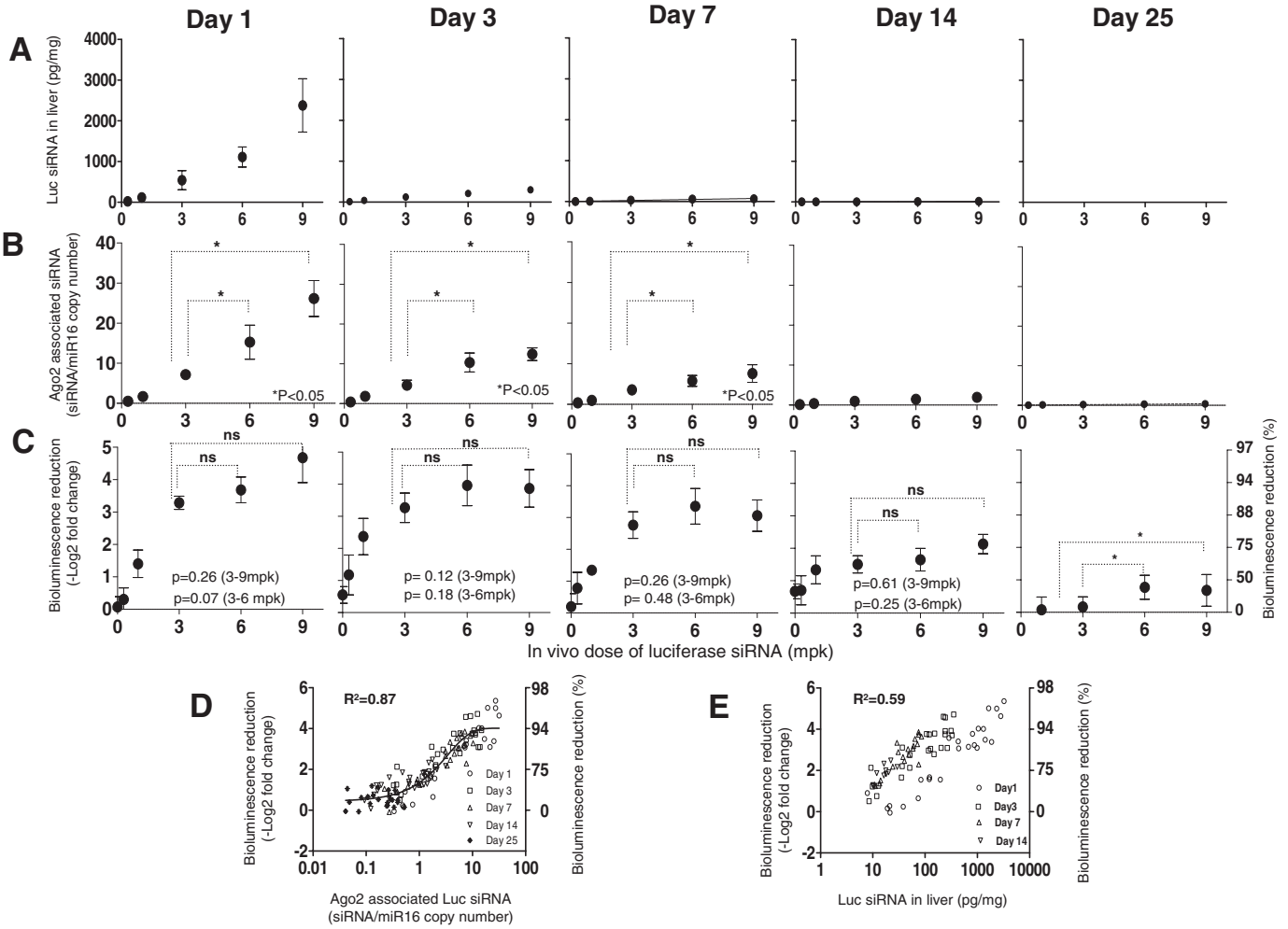


**Fig. 2.** Quantitation of luciferase siRNA in the liver or associated with Ago2 and the relationship to luciferase protein silencing measured by bioluminescence. Mice were intravenously injected with 0.3, 1, 3, 6, or 9 mg/kg LNP-formulated luciferase siRNA. Mice were imaged and sacrificed, and liver tissues were collected at days 1, 3, 7, 14, and 25 after dosing. A, Dose-dependent increases of total siRNA in the liver were observed followed by rapid clearance. Data represent the mean ± S.D. based on five mice per group. At day 3 and beyond for all doses, the error bars are smaller than the data symbols. B, Ago2-associated luciferase siRNA is dose-dependent and persists over time. Luciferase siRNA associated with Ago2 is presented as the copy number ratio of siRNA guide strand to miR16 at each dose and time point (mean ± S.D.; $n = 5$). C, potent and sustained luciferase protein silencing. Relative bioluminescence ($-\log_2$-fold change or percentage reduction) was used to monitor the silencing of luciferase at various doses (milligrams per kilogram) and time (days). Data represent the mean ± S.D. based on five mice per group. D, a correlation between luciferase protein silencing and the amount of siRNA associated with Ago2 was observed across all doses and time points ($R^2 = 0.87$; $n = 125$). Relative bioluminescence is presented as $-\log_2$-fold change or percentage of reduction and luciferase. siRNA associated to Ago2 is presented as the copy number ratio of siRNA guide strand to miR16 at each dose and time point. The line corresponds to a symmetrical sigmoidal fitted curve. Each data point represents individual mouse values. E, relationship between luciferase-protein silencing (relative bioluminescence; $-\log_2$-fold change or percentage reduction) and the concentration of total siRNA in liver (picograms per milligram). The coefficient of determination is 0.59 ($R^2 = 0.59$; $n = 105$). The line represents the symmetrical sigmoid fitted curve. The amount of siRNA in the liver at day 25 was below level of detection.

of Ago2 immunoprecipitation was evaluated by immunoblotting and shown to be similar (Supplemental Fig. 4).

**The Time Course of Biodistribution, RISC Loading, and Bioluminescence Measured at Early Time Points after Luciferase siRNA Administration.** We evaluated the early kinetics of gene silencing from 5 min to 72 h after single administration of one dose of luciferase siRNA (Fig. 4) or escalating doses of siRNA (Fig. 5; Supplemental Fig. 5).

Highest plasma concentrations were observed at 5 min after siRNA injection, which decreased 10-fold within an

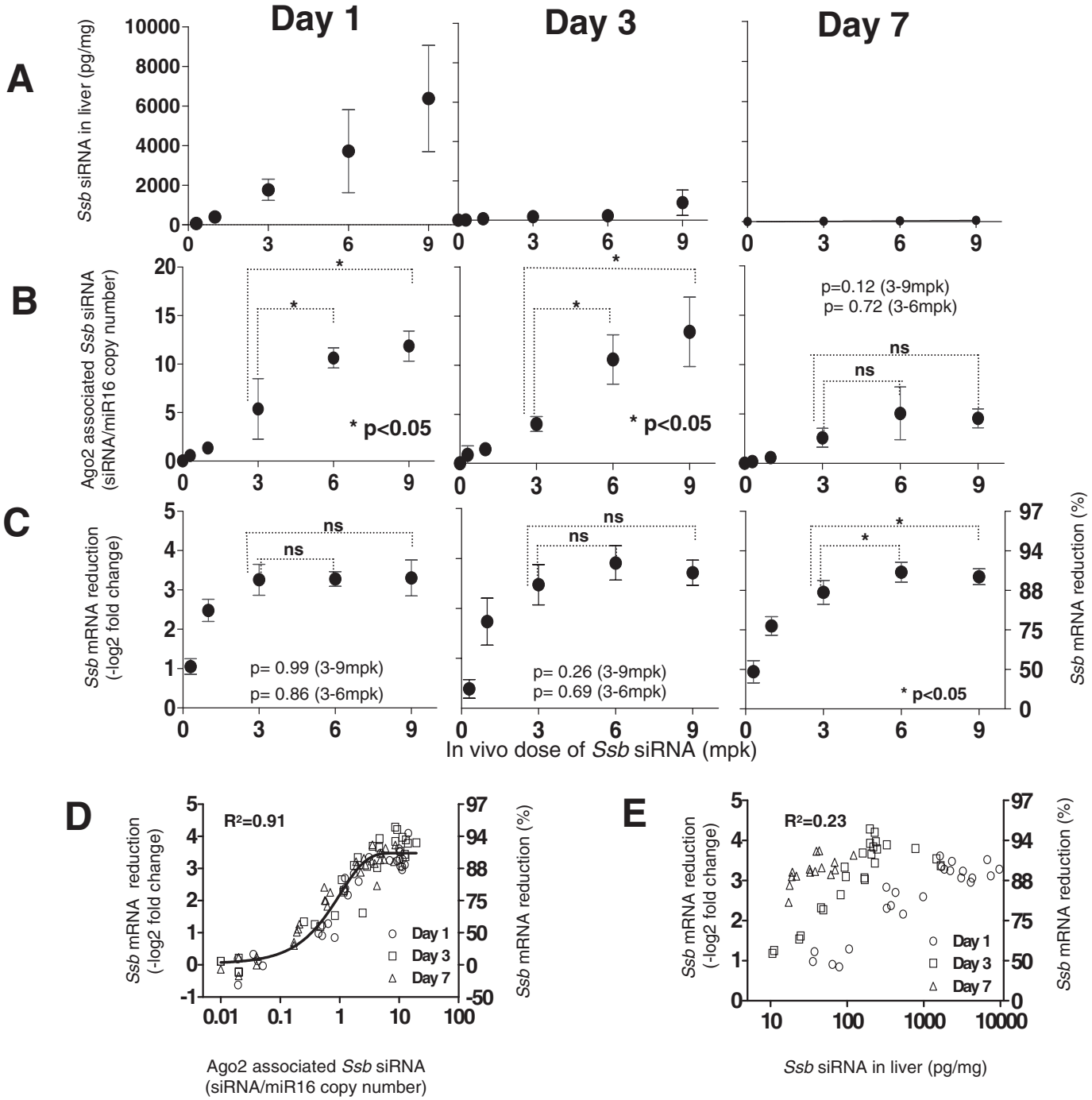


**Fig. 3.** Ssb mRNA silencing correlated with the amount of siRNA bound to Ago2. Mice were intravenously injected with 0.3, 1, 3, 6, or 9 mg/kg LNP-formulated siRNA-targeting Ssb mRNA. Mice were sacrificed and livers were collected at days 1, 3, and 7 after dosing. Two independent studies showed similar results. A, total Ssb siRNA in the liver (pg/mg). B, Ago2-associated Ssb siRNA in the liver. The amount of Ssb siRNA associated with Ago2 is presented as the copy number ratio of Ssb siRNA guide strand to miR16 associated with Ago2 (mean ± S.D.; five mice per group) at each dose (milligrams per kilogram) and time point (days). C, dose-dependent time course of Ssb mRNA silencing. Ssb mRNA reduction was evaluated by real-time qPCR as described under *Materials and Methods* and presented as $-\log_2$-fold change or percentage of reduction (mean ± S.D.; five mice per group). D, a direct correlation between Ssb mRNA silencing and the amount of Ssb siRNA associated with Ago2 was observed across all doses and time points ($R^2 = 0.91$; $n = 90$ mice). The line corresponds to a symmetrical sigmoidal fitted curve. Each data point represents individual mouse value. E, weaker correlation between Ssb mRNA inhibition and the concentration of siRNA in liver ($R^2 = 0.23$; $n = 80$ mice). Each data point represents individual mouse value.

hour. (Fig. 4, A and B; Supplemental Fig. 5A). In liver, the amount of siRNA reached maximum levels at 10 to 20 min and decreased to 1 and 0.2% of the initial siRNA in liver by 24 h and 72 h, respectively (Fig. 4, A and B; Supplemental Fig. 5B). Although the total amounts of siRNA in the liver and the plasma were declining, a time-dependent increase of Ago2-bound siRNA was observed from 5 min after dosing that gradually increased to maximum levels at 6 h (Fig. 4; Supplemental Fig. 5, A–C). The Ago2 binding was followed by detectable mRNA silencing 2 h later (Supplemental Fig. 5D) and protein silencing 6 h later (Fig. 4D; Supplemental Fig. 5E). The time difference between the initial luciferase mRNA and protein knockdown is consistent with 3- to 4-h half-life of the luciferase protein (Leclerc et al., 2000). Tukey's multiple comparison test demonstrates lack of statistical significance among PBS-, Ssb-, and UC3 siRNA-treated groups at 6 h after treatment (Supplemental Fig. 6). There was no significant difference in bioluminescent signal at 6 h between mice treated with PBS and mice treated with irrelevant siRNA (Ssb or UC3), which demonstrates the lack of a nonspecific effect on luminescence at early time points (Supplemental Fig. 6). The luciferase siRNA treated group was statistically significantly different from the control groups ($p < 0.05$).

We observed that after siRNA injection, Ago2-siRNA complex formation was maximum at 6 h, followed by maximum protein silencing between 24 and 72 h (Fig. 4, C and D). These data demonstrate that the maximum amount of siRNA bound to Ago2 precedes the maximum reduction of bioluminescence. The complete early time data set analyzed across all time points further confirmed the relationship between in vivo target silencing and Ago2-bound siRNA in the liver ($R^2 = 0.65$, $n = 135$) (Fig. 5A). In contrast, no correlation was observed between total liver siRNA concentrations and mRNA silencing (Fig. 5B). These data reveal the early progression of events between siRNA administration and its pharmacological effect in the liver and strongly suggest that Ago2-bound siRNA is a major determinant of target inhibition.

## Discussion

One of the biggest challenges in drug development is the transition of a potential therapeutic agent from preclinical research to clinical candidate selection and phase I dosing. siRNA therapeutics are no exception. Differences between RNAi mechanisms in mice and humans might make it difficult to directly translate the PK/PD relationship from mice to humans. However, knowledge of PK/PD in mice would undoubtedly provide valuable information and a possible data-driven linkage between discovery and the clinic. The current

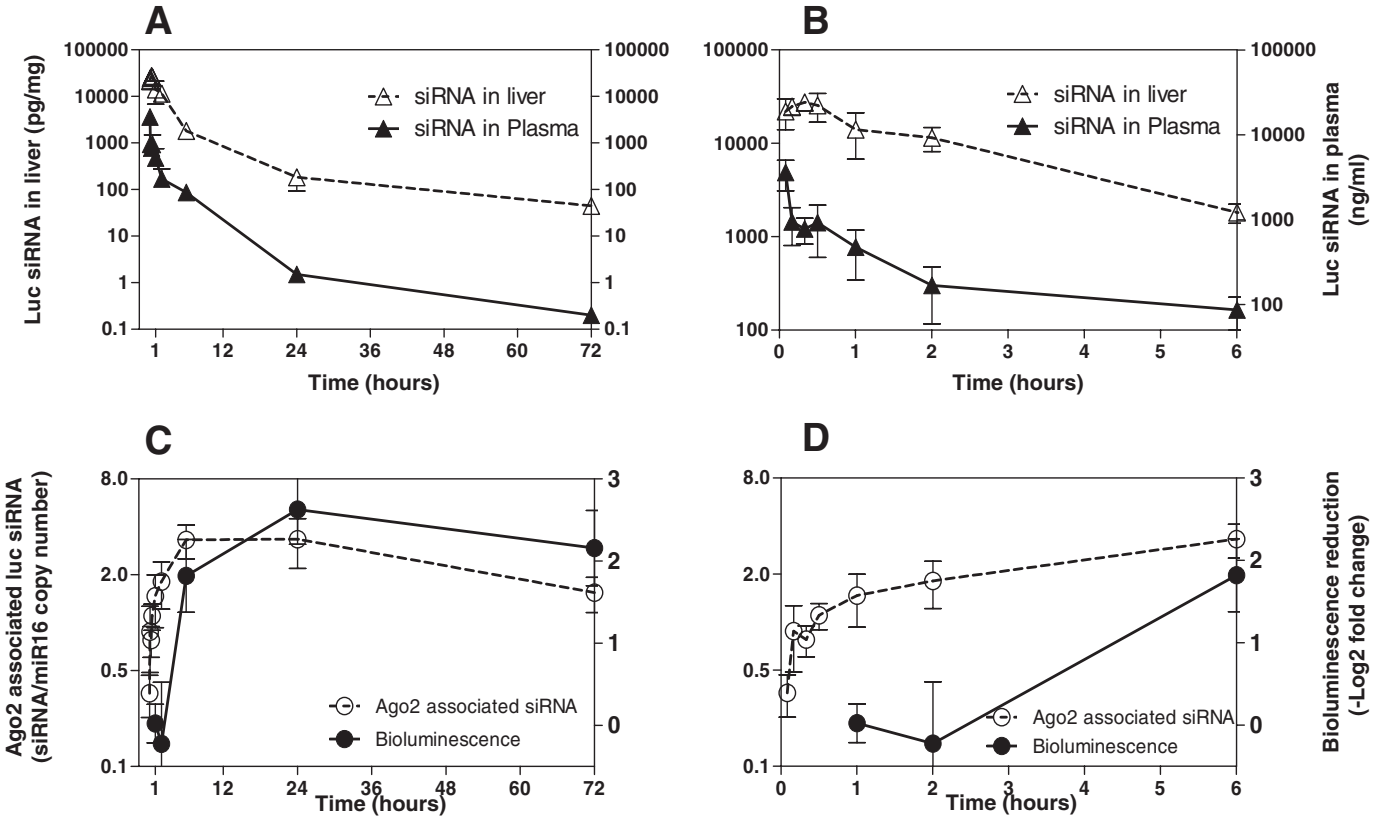


**Fig. 4.** Luciferase siRNA PK/PD relationship from 5 min to 72 h. Mice were intravenously injected with 3 mg/kg LNP-formulated luciferase siRNA or PBS. Liver samples were collected at 5, 10, 20, and 30 min and 1, 2, 6, 24, and 72 h after dosing. Each data point represents the mean value, and the error bars indicate the standard deviation based on five mice per group. A, rapid decrease of luciferase siRNA concentrations in the plasma and liver was observed from 5 min to 72 h after siRNA administration. The amount of luciferase siRNA in liver is presented as picograms per milligram. The amount of siRNA in the plasma is presented as nanograms per milliliter. B, expanded depiction of luciferase siRNA concentrations in the plasma and liver at early time points from 5 min to 6 h. C, the time profile of luciferase siRNA binding to Ago2 and luciferase protein inhibition from 5 min to 72 h. The amount of luciferase siRNA associated to Ago2 is presented as the copy number ratio of luciferase siRNA guide strand to miR16 in liver. Relative bioluminescence reduction presented as $-\log_2$-fold change relative to pretreatment level for the same mice. D, the time course of luciferase siRNA binding to Ago2 and luciferase protein inhibition from 5 min to 6 h after dosing.

lack of quantitative preclinical PK/PD studies prompted us to examine the fate and biological effect of siRNAs from 5 min to 25 days after a single intravenous administration of an LNP-formulated siRNA. We developed PK/PD relationships for two siRNAs targeting either luciferase or Ssb mRNA. Our results provide a timeline of events after siRNA injection beginning with clearance from the plasma, rapid delivery to the liver, immediate RISC loading, followed by mRNA degradation and protein inhibition. Weak relationship between the total amount of siRNA and mRNA knockdown in liver was seen at early time points. Total siRNA in the liver decreased rapidly after siRNA dosing. Although the majority of siRNA delivered to the liver did not load to RISC and was subsequently cleared from the liver, the amount of Ago2-bound siRNA complexes increased in a dose-dependent fashion and strongly correlated with increased target silencing, suggesting that the number of Ago2-siRNA complexes is a key determinant of RNAi-mediated gene silencing in mice. These data also suggest that our current delivery is inefficient and requires excess input to achieve maximum mRNA silencing.

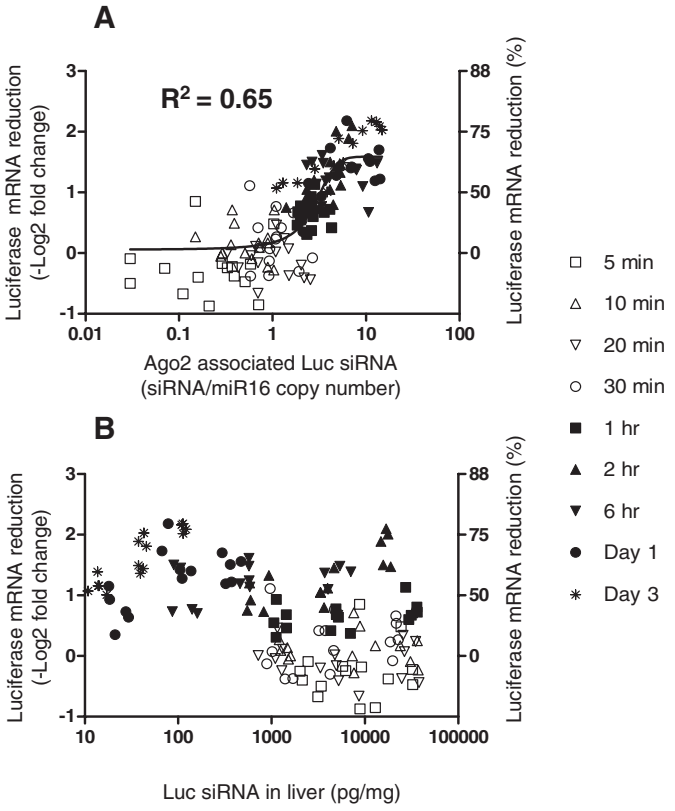


**Fig. 5.** Direct correlation was observed between mRNA reduction and Ago2-associated luciferase siRNA across time points from 5 min to 72 h but not with total luciferase siRNA in liver. Five mice per group were injected with 0.3, 1, or 3 mg/kg luciferase siRNA. PBS-treated mice were used as controls. After siRNA injection, all mice were imaged and sacrificed for liver harvesting at 5, 10, 20, and 30 min and 1, 2, 6, 24, and 72 h after dosing. At each time point, the amount of guide strand siRNA bound to Ago2, the total siRNA, and mRNA reduction in the liver tissue were determined. Luciferase mRNA reduction is presented as $-\log_2$-fold change or as percentage luciferase mRNA reduction. A, a correlation between luciferase mRNA reduction and the amount of luciferase guide strand associated with Ago2 can be observed across all doses and time points ($R^2$ = 0.65, $n$ = 135). The amount of siRNA bound to Ago2 is presented as the copy number ratio of luciferase siRNA guide strand to miR16. Each data point represents an individual mouse. The line represents a symmetrical sigmoidal fitted curve. B, no relationship between luciferase mRNA silencing and the total amount of siRNA in mouse liver was observed across different doses and times (5 min–72 h).

The value of PK/PD relationships is to inform multiple key drug development goals, including an understanding of the underlying mechanism of action and a prediction of in vivo potency and durability (Meibohm and Derendorf, 2002). Our results suggest that siRNA-mediated in vivo activity and duration of action are based on the number of Ago2-siRNA complexes and the stability of the complex over time. Our in vivo data suggesting that 280 to 1260 Ago2-siRNA complexes per cell are sufficient for 50% silencing correspond remarkably well with cell-based microinjection experiments using luciferase plasmid and varying concentrations of siRNAs (Veldhoen et al., 2006). Ninety percent inhibition of Ssb or luciferase mRNA required approximately 2400 and 7600 Ago2-siRNA complexes, respectively. It is noteworthy that the number of Ago2-siRNA complexes required for 50% silencing of the endogenous Ssb gene is 4-fold less than the number of complexes needed to silence the luciferase transgene. It is likely that the absolute number of Ago2-siRNA complexes required for 50% silencing of other targets will also vary based on the siRNA molecule, turnover of the Ago2 complex in various organs, target mRNA half-life, mRNA expression levels, cell division and turnover, or a combination thereof (Bartlett and Davis, 2006; Adams et al., 2009).

The duration of action of an siRNA is determined by maximum target mRNA silencing and PD half-life of the pharmacologic effect measured. Maximum luciferase-target silencing was dose-dependent, whereas the PD half-life, as measured by the recovery of luciferase-mediated bioluminescence over time, was not significantly different for each treatment group. These results imply that the biological half-life of the Ago2-siRNA complex is similar over a range of siRNA concentrations, suggesting that continuous reloading of Ago2 or loading of newly synthesized Ago2 with an intracellular pool of siRNA is unlikely; otherwise, it would be expected that increasing doses of siRNAs might result in an extended PD half-life. Alternatively, the maximum silencing and half-life of the Ago2-siRNA complex could be solely dependent on the intrinsic properties of the siRNA. For instance, chemically modified siRNAs that improve serum stability have been observed to extend the duration of action compared with unmodified siRNA (Morrissey et al., 2005a,b). Moreover, siRNA chemical modifications that improve the binding on-rate to Ago2 might be expected to improve activity, whereas modifications that slow Ago2 off-rates may result in enhanced durability. Crystal structures of the eukaryotic Ago2 middle domain (Mid) (Boland et al., 2010) that binds the 5′ phosphate of the guide strand and PIWI/Argonaute/Zwille (PAZ) domain (Somoza et al., 2010) that binds the 3′ end of the guide strand provide opportunities for structure-based design of chemically modified siRNAs. In fact, replacement of the conventional two-base deoxythymidine overhang on the 3′ end of the guide strand with two uridines containing 2′-*O*-methyl modifications improved siRNA duration (Strapps et al., 2010). Dramatic improvements in the equilibrium-binding constant between a siRNA and Ago2 using chemical modifications may increase both potency and durability, resulting in more convenient dose and dose schedules, improved safety profiles, and better doctor and patient acceptance of this new treatment modality.

Quantitative PK/PD analysis of new therapeutic modali-

ties such as siRNAs can address potential safety concerns. In particular, there is a concern that the use of therapeutic siRNAs will be limited to life-threatening diseases because siRNAs have the potential to saturate RISC machinery, resulting in toxicity (Grimm et al., 2006). Over a range of 1 to 6 mg/kg siRNA doses tested, we failed to observe any saturation of Ago2 binding with either the luciferase or Ssb siRNA despite attaining substantial mRNA target inhibition at the identical siRNA doses. These results raise the possibility that luciferase protein inhibition or Ssb mRNA knockdown is saturated by limitations other than Ago2 loading. We did not see a statistically significant increase of the Ago2 bound siRNA from 6 to 9 mg/kg. It is possible that Ago2 saturation occurs at 9 mg/kg dose. However, it remains probable that more than 1.5-fold increase in the dose is required to reach significance. Unfortunately, we are unable to raise the dose to test this, because a 12 mg/kg or higher dose induces in vivo toxicity with the current vehicle.

The lack of siRNA-bound Ago2 saturation at 1 to 6 mg/kg siRNA doses suggests that Ago2 binding is not a limiting step in reaching maximum inhibition of gene expression with our current delivery vehicle. This observation is consistent with the ability to perform combination therapy with two or more siRNAs (Love et al., 2010). One possible explanation for the failure to observe Ago2 binding saturation is that the expression of Ago2 is up-regulated in a dose-dependent fashion after siRNA injection. However, analysis of Ago2 mRNA levels after escalating doses of luciferase or Ssb siRNA administration failed to reveal any significant increase of Ago2 mRNA expression in the liver (data not shown). In addition, our results and those previously reported (John et al., 2007) demonstrated that comparable levels of miR16 bound to Ago2 are seen in the livers of mice given increasing doses of siRNAs. The mechanisms of RNAi are not completely understood today, and other regulatory mechanisms might account for the lack of obvious Ago2 saturation.

The ability to reach substantial target inhibition before Ago2 binding saturation has important implications for optimal dose selection and schedule. The minimal siRNA dose that results in maximal therapeutic effect is the goal. Of course, convenience of the dose schedule will play a role in the selection of the dose; however, increasing siRNA doses that do not enhance duration of action could result in unanticipated toxicities and confound the clinical benefits mediated by the siRNA. Off-target effects have been observed to increase with increasing siRNA concentrations (Martin et al., 2007). Fortunately, chemical modifications such as 2′-*O*-methyl modification at position 2 of the siRNA guide strand can mitigate many off-target RNA-silencing effects without affecting siRNA potency (Jackson et al., 2006). Nonetheless, the minimal siRNA dose and schedule that reaches a threshold number of Ago2-siRNA complexes resulting in therapeutic benefit could provide the maximum therapeutic index. Further studies addressing the RNAi mechanism of action will be needed to clarify this important point.

Taken together, our data provide a quantitative in vivo PK and PD relationship for LNP-delivered siRNAs. These detailed kinetic studies should aid in selecting potent, chemically modified siRNAs, optimizing siRNA delivery vehicles, mitigating off-target effects, and developing phase I dosing regimens with the ultimate goal of streamlining the clinical development and success of candidate siRNA molecules.

**Acknowledgments**

We thank Dr. Amy O. Johnson-Levonas and Kathleen Newcomb of Merck Sharp and Dohme Corp. for their editorial and writing support.

**Authorship Contributions**

*Participated in research design:* Wei, Cancilla, Flanagan, and Kuklin.

*Conducted experiments:* Wei, Jones, Kang, Card, Krimm, Hancock, Payson, and Dubinina.

*Performed data analysis:* Wei, Jones, Card, Krimm, Stroh, Buchard, and Kuklin.

*Wrote or contributed to the writing of the manuscript:* Wei, Jones, Card, Pei, Ason, Cancilla, Stroh, Buchard, Sachs, Hochman, Flanagan, and Kuklin.

**References**

Adams BD, Claffey KP, and White BA (2009) Argonaute-2 expression is regulated by epidermal growth factor receptor and mitogen-activated protein kinase signaling and correlates with a transformed phenotype in breast cancer cells. *Endocrinology* **150:**14–23.

Bartlett DW and Davis ME (2006) Insights into the kinetics of siRNA-mediated gene silencing from live-cell and live-animal bioluminescent imaging. *Nucleic Acids Res* **34:**322–333.

Bartlett DW and Davis ME (2007) Effect of siRNA nuclease stability on the in vitro and in vivo kinetics of siRNA-mediated gene silencing. *Biotechnol Bioeng* **97:**909–921.

Boland A, Tritschler F, Heimstädt S, Izaurralde E, and Weichenrieder O (2010) Crystal structure and ligand binding of the MID domain of a eukaryotic Argonaute protein. *EMBO Rep* **11:**522–527.

Chen C, Ridzon DA, Broomer AJ, Zhou Z, Lee DH, Nguyen JT, Barbisin M, Xu NL, Mahuvakar VR, Andersen MR, et al. (2005) Real-time quantification of microRNAs by stem-loop RT-PCR. *Nucleic Acids Res* **33:**e179.

Davis ME, Zuckerman JE, Choi CH, Seligson D, Tolcher A, Alabi CA, Yen Y, Heidel JD, and Ribas A (2010) Evidence of RNAi in humans from systemically administered siRNA via targeted nanoparticles. *Nature* **464:**1067–1070.

DeVincenzo J, Cehelsky JE, Alvarez R, Elbashir S, Harborth J, Toudjarska I, Nechev L, Murugaiah V, Van Vliet A, Vaishnaw AK, et al. (2008) Evaluation of the safety, tolerability and pharmacokinetics of ALN-RSV01, a novel RNAi antiviral therapeutic directed against respiratory syncytial virus (RSV). *Antiviral Res* **77:**225–231.

Elbashir SM, Harborth J, Lendeckel W, Yalcin A, Weber K, and Tuschl T (2001) Duplexes of 21-nucleotide RNAs mediate RNA interference in cultured mammalian cells. *Nature* **411:**494–498.

Gabrielsson J, Dolgos H, Gillberg PG, Bredberg U, Benthem B, and Duker G (2009) Early integration of pharmacokinetic and dynamic reasoning is essential for optimal development of lead compounds: strategic considerations. *Drug Discov Today* **14:**358–372.

Gilmore IR, Fox SP, Hollins AJ, and Akhtar S (2006) Delivery strategies for siRNA-mediated gene silencing. *Curr Drug Deliv* **3:**147–155.

Grimm D, Streetz KL, Jopling CL, Storm TA, Pandey K, Davis CR, Marion P, Salazar F, and Kay MA (2006) Fatality in mice due to oversaturation of cellular microRNA/short hairpin RNA pathways. *Nature* **441:**537–541.

Jackson AL, Burchard J, Leake D, Reynolds A, Schelter J, Guo J, Johnson JM, Lim L, Karpilow J, Nichols K, et al. (2006) Position-specific chemical modification of siRNAs reduces "off-target" transcript silencing. *Rna* **12:**1197–1205.

John M, Constien R, Akinc A, Goldberg M, Moon YA, Spranger M, Hadwiger P, Soutschek J, Vornlocher HP, Manoharan M, et al. (2007) Effective RNAi-mediated gene silencing without interruption of the endogenous microRNA pathway. *Nature* **449:**745–747.

Leclerc GM, Boockfor FR, Faught WJ, and Frawley LS (2000) Development of a destabilized firefly luciferase enzyme for measurement of gene expression. *Biotechniques* **29:**590–591, 594–596, 598 passim.

Lima WF, Wu H, Nichols JG, Sun H, Murray HM, and Crooke ST (2009) Binding and cleavage specificities of human Argonaute2. *J Biol Chem* **284:**26017–26028.

Livak KJ and Schmittgen TD (2001) Analysis of relative gene expression data using real-time quantitative PCR and the $2^{(-\Delta\Delta C_T)}$ method. *Methods* **25:**402–408.

Love KT, Mahon KP, Levins CG, Whitehead KA, Querbes W, Dorkin JR, Qin J, Cantley W, Qin LL, Racie T, et al. (2010) Lipid-like materials for low-dose, in vivo gene silencing. *Proc Natl Acad Sci USA* **107:**1864–1869.

Martin SE, Jones TL, Thomas CL, Lorenzi PL, Nguyen DA, Runfola T, Gunsior M, Weinstein JN, Goldsmith PK, Lader E, et al. (2007) Multiplexing siRNAs to compress RNAi-based screen size in human cells. *Nucleic Acids Res* **35:**e57.

Matranga C, Tomari Y, Shin C, Bartel DP, and Zamore PD (2005) Passenger-strand cleavage facilitates assembly of siRNA into Ago2-containing RNAi enzyme complexes. *Cell* **123:**607–620.

Meibohm B and Derendorf H (2002) Pharmacokinetic/pharmacodynamic studies in drug product development. *J Pharm Sci* **91:**18–31.

Meister G, Landthaler M, Patkaniowska A, Dorsett Y, Teng G, and Tuschl T (2004) Human Argonaute2 mediates RNA cleavage targeted by miRNAs and siRNAs. *Mol Cell* **15:**185–197.

Morrissey DV, Blanchard K, Shaw L, Jensen K, Lockridge JA, Dickinson B, McSwiggen JA, Vargeese C, Bowman K, Shaffer CS, et al. (2005a) Activity of stabilized short interfering RNA in a mouse model of hepatitis B virus replication. *Hepatology* **41:**1349–1356.

Morrissey DV, Lockridge JA, Shaw L, Blanchard K, Jensen K, Breen W, Hartsough K, Machemer L, Radka S, Jadhav V, et al. (2005b) Potent and persistent in vivo anti-HBV activity of chemically modified siRNAs. *Nat Biotechnol* **23:**1002–1007.
Parker JS, Roe SM, and Barford D (2006) Molecular mechanism of target RNA transcript recognition by Argonaute-guide complexes. *Cold Spring Harb Symp Quant Biol* **71:**45–50.
Pei Y, Hancock PJ, Zhang H, Bartz R, Cherrin C, Innocent N, Pomerantz CJ, Seitzer J, Koser ML, Abrams MT, et al. (2010) Quantitative evaluation of siRNA delivery in vivo. *RNA* **16:**2553–2563.
Pei Y and Tuschl T (2006) On the art of identifying effective and specific siRNAs. *Nat Methods* **3:**670–676.
Safran M, Kim WY, Kung AL, Horner JW, DePinho RA, and Kaelin WG Jr (2003) Mouse reporter strain for noninvasive bioluminescent imaging of cells that have undergone Cre-mediated recombination. *Mol Imaging* **2:**297–302.
Scherr M and Eder M (2007) Gene silencing by small regulatory RNAs in mammalian cells. *Cell Cycle* **6:**444–449.
Sepp-Lorenzino L and Ruddy M (2008) Challenges and opportunities for local and systemic delivery of siRNA and antisense oligonucleotides. *Clin Pharmacol Ther* **84:**628–632.
Somoza A, Terrazas M, and Eritja R (2010) Modified siRNAs for the study of the PAZ domain. *Chem Commun* (*Camb*) **46:**4270–4272.
Strapps WR, Pickering V, Muiru GT, Rice J, Orsborn S, Polisky BA, Sachs A, and Bartz SR (2010) The siRNA sequence and guide strand overhangs are determinants of in vivo duration of silencing. *Nucleic Acids Res* **38:**4788–4797.
Tang F, Hajkova P, O'Carroll D, Lee C, Tarakhovsky A, Lao K, and Surani MA (2008) MicroRNAs are tightly associated with RNA-induced gene silencing complexes in vivo. *Biochem Biophys Res Commun* **372:**24–29.
Tao W, Davide JP, Cai M, Zhang GJ, South VJ, Matter A, Ng B, Zhang Y, and Sepp-Lorenzino L (2010) Noninvasive imaging of lipid nanoparticle-mediated systemic delivery of small-interfering RNA to the liver. *Mol Ther* **18:**1657–1666.
Tuschl T (2001) RNA interference and small interfering RNAs. *Chembiochem* **2:**239–245.
Vaishnaw AK, Gollob J, Gamba-Vitalo C, Hutabarat R, Sah D, Meyers R, de Fougerolles T, and Maraganore J (2010) A status report on RNAi therapeutics. *Silence* **1:**14.
Veldhoen S, Laufer SD, Trampe A, and Restle T (2006) Cellular delivery of small interfering RNA by a non-covalently attached cell-penetrating peptide: quantitative analysis of uptake and biological effect. *Nucleic Acids Res* **34:**6561–6573.
Watts JK, Deleavey GF, and Damha MJ (2008) Chemically modified siRNA: tools and applications. *Drug Discov Today* **13:**842–855.
Willmann JK, van Bruggen N, Dinkelborg LM, and Gambhir SS (2008) Molecular imaging in drug development. *Nat Rev Drug Discov* **7:**591–607.
Wincott FE (2001) Strategies for oligoribonucleotide synthesis according to the phosphoramidite method. *Curr Protoc Nucleic Acid Chem* **Chapter 3:**Unit 3.5.
Zou Y, Tiller P, Chen IW, Beverly M, and Hochman J (2008) Metabolite identification of small interfering RNA duplex by high-resolution accurate mass spectrometry. *Rapid Commun Mass Spectrom* **22:**1871–1881.

**Address correspondence to:** Nelly A. Kuklin, Sirna Therapeutics, a wholly owned subsidiary of Merck and Co Inc., 1700 Owens St., 4th Floor, San Francisco, CA 94158. E-mail: nelly_kuklin@merck.com